Progress In Electromagnetics Research C, Vol. 26, 97–110, 2012

DESIGN OF A WIDE BAND EIGHT-WAY COMPACT SIW POWER COMBINER FED BY A LOW LOSS GCPW-TO-SIW TRANSITION

R. Kazemi[1, *], R. A. Sadeghzadeh[1], and A. E. Fathy[2]

[1]Faculty of Electrical and Computer Engineering, K. N. Toosi University of Technology, Tehran 1431714191, Iran

[2]Electrical Engineering and Computer Science Department, University of Tennessee, Knoxville 37996, TN, USA

Abstract—Ultra wideband components have been developed using SIW technology. The various newly developed components include a GCPW transition, Y and T-junctions. The GCPW transition covers over 10 GHz bandwidth with less than 0.4 dB insertion loss. The optimized T and Y-junctions have relatively wide bandwidths of greater than 40% that have less than 0.6 dB insertion loss. The developed transition was utilized to design an X-band eight-way power divider that demonstrated excellent performance over a 4 GHz bandwidth with less than $\pm 4^\circ$ and ± 0.9 dB phase and amplitude imbalance, respectively. Theoretical and experimental results are presented and compared with previously designed SIW power dividers. The developed SIW power divider has a low profile and is particularly suitable for circuits' integration.

1. INTRODUCTION

Waveguide power dividers are widely used in many microwave and millimeter-wave systems to design various subsystems such as multiplexers, couplers, antenna feeding systems, and many other components for their extremely low loss and high power handling capabilities [1]. However, Conventional waveguide components are typically bulky and expensive; and difficult to integrate with other microwave and millimeter wave planar circuits. On the other hand, microstrip lines are compact and low cost, and have been widely used, but they are relatively lossy. However, they are convenient for planar

Received 9 November 2011, Accepted 4 December 2011, Scheduled 12 December 2011

* Corresponding author: Robab Kazemi (r.kazemi@ee.kntu.ac.ir).

circuits and subsystems like feed networks. For example, Yang et al. [2] utilized a multitude of wide band Wilkinson combiners to cover the 8–12 GHz bandwidth, but its overall insertion loss was unacceptably high at over 3.5 dB.

Recently, Hao et al. and Germain et al. [1, 3] have utilized an alternative low cost technology to build a wide range of mm-wave components. The technology is based on using printed circuit boards to emulate waveguides and is called substrate integrated waveguides (SIW), and is known for its numerous advantages such as relatively high Q, ease of integration, compact size, and low cost. The developed SIW components have gone through significant performance improvement over the years through novel design additions. Various SIW power dividers have been studied like in [1, 3], and [4] and relatively good results have been already reported. For example, Hao et al. in [1, 4] utilized a SIW binary feed network that showed an improved performance, but its 2.5 dB insertion loss is still relatively high and does not cover the entire X-band frequency range (8–12 GHz). Similarly, Yang et al. [5] developed an 8 way SIW power divider, but its insertion loss is also relatively high (2.5 dB) over 9–11 GHz frequency band, but definitely there is still a room for further development. A comparison between these previously developed dividers is shown in Table 1.

Table 1. Comparison between different dividers.

	Y. Yang	S. Yang	Hao
# ways	16	8	16
Technology	Microstrip	SIW	Microstrip
Bandwidth/Frequency Range (GHz)	4 GHz (8–12)	2 GHz (9–11)	3.5 GHz (10–13.5)
I.L. (dB)	3.5	2.5	2.5

2. DESIGN OF AN ULTRA WIDEBAND GCPW-TO-SIW TRANSITION

In designing SIW, the diameter d of the vias, the pitch spacing between the vias p, and the spacing a between the two vias rows are our design degrees of freedom. Based on extensive simulation results of different SIW geometries, where $a/p > 2.5$, it was concluded that the post diameter d and the pitch p should be selected in the range of $d < \lambda_g/5$ and $p \leq 2d$, respectively to minimize leakage loss [6], while complying with fabrication constraints. When a/p becomes large

or p/d becomes small, the leaky wave radiating from gaps between metallic vias decreases and the SIW guiding wave property can be emulated using an equivalent metallic waveguide [7]. To simplify our analysis, we adapted this equivalence and selected $d = 0.5\,\text{mm}$ and $p = 0.9\,\text{mm}$ for designing the various proposed SIW structures in this paper.

Here, a relatively thick substrate is used to lower the conductor loss of the SIW structure. SIW is typically fed by a microstrip [8–12], however, for a thick substrate, a $50\,\Omega$ microstrip feed line will be very wide and would excite higher order modes with the potential to radiate. As an alternative, we have developed a grounded coplanar waveguide (GCPW) feed for a smoother transition [13, 14].

Typically a GCPW to SIW transition is comprised of two sections, a coupling slot section followed by a transformer section. To achieve a relatively wide band transition, both the coupling slot and its impedance transformer can be integrated into one tapered coupling slot [5]. To further improve such feed, the side walls of the waveguide are elegantly tapered along the triangle-shaped coupling slot in such a way that the direction of the electric field on the coupling slot is always perpendicular to the SIW sidewalls as shown in Figure 1(a).

Additional performance improvement can be achieved upon strategically placing metalized vias along the GCPW to cancel the parallel plate modes in the GCPW line, and stop the waveguide modes entering the GCPW from the SIW side. In our design, these metallic posts have been positioned in two rows near the GCPW to avoid any resonance within the operating band, and the distance between them is used effectively to suppress any leaky modes; thus sustaining single-mode propagation over the operating band. Meanwhile, to assure a

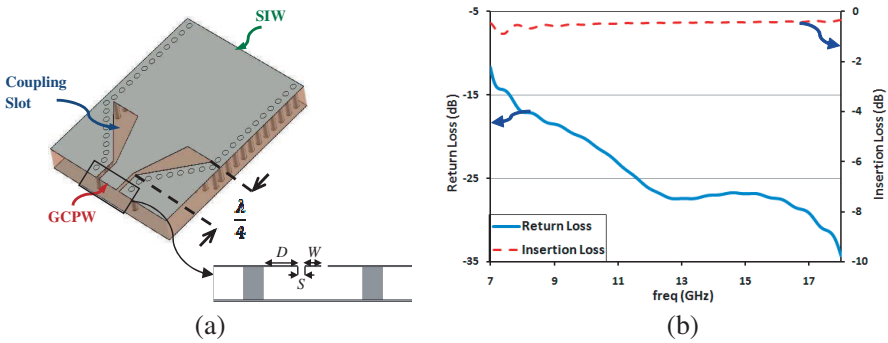

Figure 1. (a) Novel UWB GCPW to SIW transition. (b) Simulated return loss and insertion loss of transition.

single mode operation in the CPW side, we have satisfied the following condition [15]

$$W + 2S + 2D < \frac{c}{2f_{\max}\sqrt{\varepsilon_r}} \tag{1}$$

where W, S, and D are the strip width, gap between the line and adjacent ground plane, and the distance between the gap and vias, respectively, as shown in Figure 1(a), and $f_{\max}$ is the maximum frequency of operation; given that the first higher order mode has a cut-off frequency similar to that of the TE_{10} mode in a rectangular waveguide. Subsequently, it was predicted that the optimized length of the taper slot is $\lambda/4$ at the center frequency ($f_0 = 10\,\text{GHz}$) to achieve a wider bandwidth, where $\lambda = \lambda_o/\sqrt{\varepsilon_r}$ [16].

Meanwhile, the design of the SIW transition involves the selection of the substrate properties (i.e., thickness and dielectric constant) which presumably would affect its return loss and insertion loss performance. Therefore, to obtain a wide band low insertion loss design, we ran an extensive parametric study using CST simulation tool where the substrate thickness was varied in discrete steps from 0.5 to 3 mm for a family of dielectric constant substrates namely; 2.2, 3.38, and 4.5. Figure 2 shows the simulated fractional bandwidth, reflection and transmission coefficient of a back-to-back GCPW-SIW transition versus substrate thickness (normalized to the center wavelength) for these different substrates. As seen in Figure 2(a), use of a substrate with a high dielectric constant tends to generally increase the transition's fractional bandwidth. Meanwhile, increasing the substrate thickness would decrease the insertion loss of the transition as depicted in Figure 2(b).

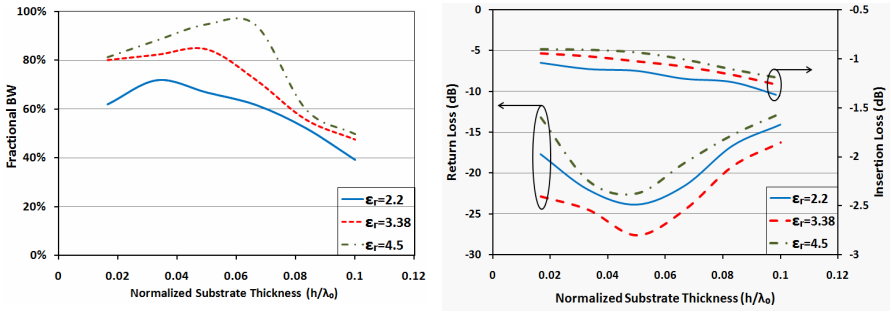

Figure 2. Design charts showing: (a) 10-dB return loss-fractional bandwidth and (b) the transmission and reflection coefficient of a back-to-back 2″ length transition.

Based on our simulation, a wide bandwidth of more than 80% is predicted for the proposed triangle slot transition, as shown in Figure 1(b); Upon using $\varepsilon_r = 3.38$ and $h = 0.05\lambda_o$, better than 0.8 dB insertion loss and 20 dB return loss are obtained for a back-to-back transition over a 10 GHz frequency range. For design validation, a back-to-back transition was fabricated using a 1.524 mm thick substrate ($h = 0.05\lambda_o$) with $\varepsilon_r = 3.38$ and $\tan\delta = 0.0027$ (RO4003c) in two different lengths, 53 mm and 132 mm as shown in Figure 3. The measured insertion loss results are in very good agreement with the simulated results and show that the designed transition of a 53 mm operates over a bandwidth of 10 GHz with an insertion loss of 0.4 dB. This is a considerable improvement over the previously reported results of about 0.6 dB in [5] over 9–11 GHz and 0.7 dB in [16] at 7–9 GHz for a similar transition designed to operate over a 2 GHz bandwidth. Table 2 categorizes the simulated loss contributions due to metal, dielectric, leakage, and SMA connectors using CST simulation. As it can be

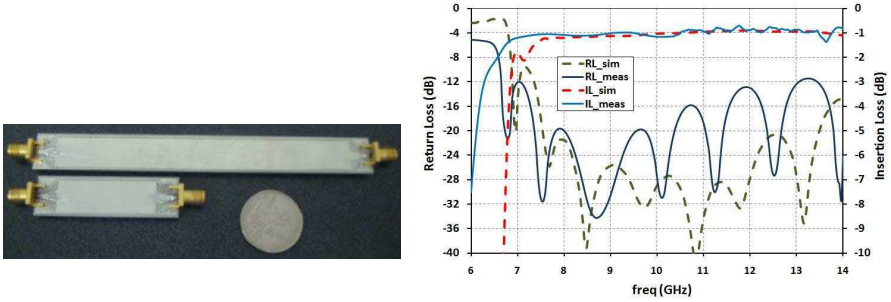

(a) (b)

Figure 3. (a) GCPW to SIW back-to-back transition. (b) Simulated and measured results of the back-to-back 2″ length transition.

Table 2. Summary of the simulated loss results in a 2″ length back-to-back transition, where we account one source of loss at a time and assume other loss contributors are lossless (ideal).

Component	Loss (dB)
Dielectric loss	0.5
Copper loss	0.07
Transition and connector loss	0.2
Leakage loss	0.11
Total loss	0.88

seen, most of the losses are due to dielectric and connector losses. Therefore, further insertion loss reduction can be achieved upon using substrates with lower loss tangents, and generally we should use high quality connectors to avoid poor mismatch at high frequencies as well.

3. POWER DIVIDER DESIGN

The developed binary feed network design is based on an extensive use of optimized T and Y junctions for conventional waveguides [17], and their implementation using SIW [18, 19] (as shown in Figure 4). In our T-junction design, the width of SIW is selected such that the center frequency of operation is right at the middle of the operating band. So we have selected $f_0 = 1.5f_c$, where $f_0 = 10\,\text{GHz}$ is the center frequency and f_c is the cut-off frequency of the TE_{10} mode. This selection renders a relatively wide bandwidth as well as a decent insertion loss performance for a single stage T-junction. Then the spacing between the combining stages is judiciously selected to achieve a wideband eight-way power divider structure. The width of the SIW structure can be calculated using the following design equations:

$$f_c(\text{TE}_{10}) = \frac{f_0}{1.5} = 6.7\,\text{GHz} \tag{2}$$

$$f_c(\text{TE}_{10}) = \frac{c}{2a\sqrt{\varepsilon_r}} \tag{3}$$

where c is the free-space EM wave velocity and ε_r is the dielectric constant of the substrate. The equivalent waveguide width "a_{eff}" is smaller than the actual lateral spacing of the posts "a" due to the vias reactive loading. However, the effective/equivalent "a" value tends to increase, whenever thinner or widely spaced posts are used. But, the wider the spacing between the posts is, the higher the leakage loss. The SIW then can no longer be used to build a feeding network

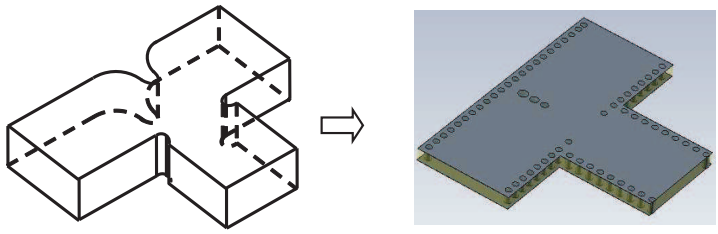

(a) (b)

Figure 4. (a) Waveguide T-junction with wedge and diaphragms. (b) The SIW counterparts of the waveguide T-junction.

for the antenna arrays due to its excessive leakage loss. Approximate design equations of the equivalent dielectric filled waveguide "a_{eff}" as a function of the diameter and spacing of the vias can be utilized according to [20] as:

$$a_{eff} = a - 1.08\frac{d^2}{p} + 0.1\frac{d^2}{a} \tag{4}$$

By using RO4003c substrate, the equivalent width of SIW is obtained as $a_{eff} = 11.8\,\text{mm}$ for $a = 12.1\,\text{mm}$. Hence, effectively the cut-off frequencies of the first and second propagating modes are 6.9 GHz and 13.8 GHz, respectively as given by (3) when "a" is replaced by "a_{eff}". In other words, with our selected SIW structure parameters, only the TE_{10} mode can propagate in the waveguide in the range of 8–12 GHz. Thus, this selection renders a relatively wide band and acceptable insertion loss performance for a T-junction with a single propagating mode and an optimization should be carried out to tradeoff between bandwidth and insertion loss.

3.1. SIW T-junction Design and Implementation

In implementing wideband SIW T-junctions, various strategies have been developed by many researchers like [2] and [3] to improve the performance of the basic T-junction shown in Figure 4(b). One, generally, can have more design degrees of freedom to obtain an arbitrary power split ratio, and achieve a good input match by using multiple posts as indicated in [2, 3]. In our equal power split design, for instance, we use three inductive posts, C2, C3, and C4 as shown in Figure 5. These posts are usually placed at the centerline of the

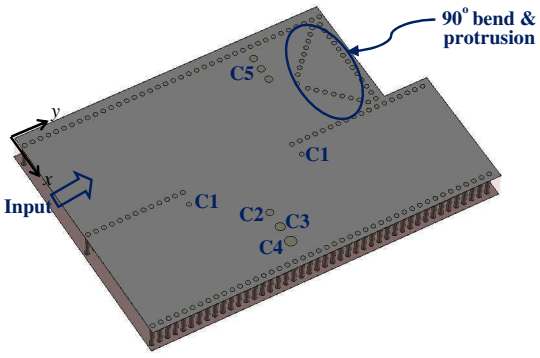

Figure 5. The geometry of the optimized T-junction with inductive posts.

input SIW, and approximately at $\lambda/4$ from the common wall of the two output ports. Meanwhile, for a smooth transition, the three posts are designed in such a way that the posts' radii increase gradually. This gradual increase of posts' radii is very similar to the shaping of the power divider's boundary for conventional waveguide power dividers recommended by [18, 19]. By optimizing the diameters and the positions of these posts, one can obtain an even output power split and achieve a good input match over a wide bandwidth. In addition to these posts, we symmetrically have added two inductive posts in the input arm C1. The diameters and positions of these posts greatly affect the splitter's input return loss. These posts act as two parallel diaphragms that compensate for the discontinuity (capacitive) effects of the bends; thus improving the coupling between the input and output ports, and improving its input return loss.

For the post and diaphragms design, we developed a set of design charts for the SIW T-junction parameters as shown in Figure 6. Both the $L1$ (distance of posts in the junction from the common sidewall of the two outputs) and $L2$ (the indent of the vias forming the diaphragms from sidewalls of the input SIW) have been optimized to achieve a perfect match at 10 GHz.

In designing an SIW bend with minimal reflections, three metallic posts "C5", and a triangular protrusion are utilized as shown in Figure 5. The initial position of the C5 posts can be chosen as $\lambda/4$ from the short circuit wall. To illustrate the effects of the three inductive posts and shaped walls on the reflection coefficient of the input port, we calculated the performance with and without posts/protrusion. As seen in Figure 7, the input return loss has been significantly improved by shaping these walls. The geometric parameters for the designed SIW T-junction are provided in Table 3.

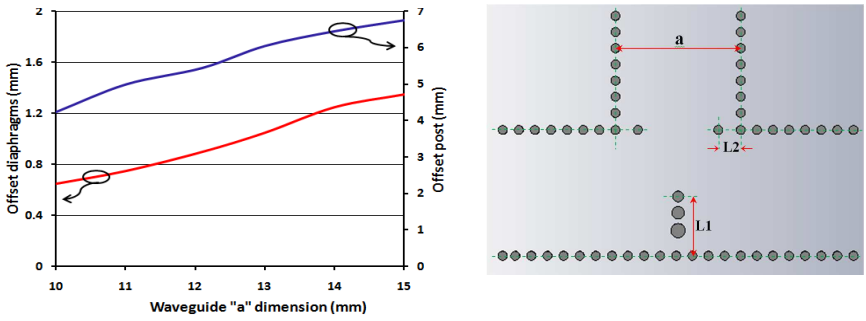

Figure 6. (a) Design charts and (b) parameters of the post and diaphragms of SIW T-junction.

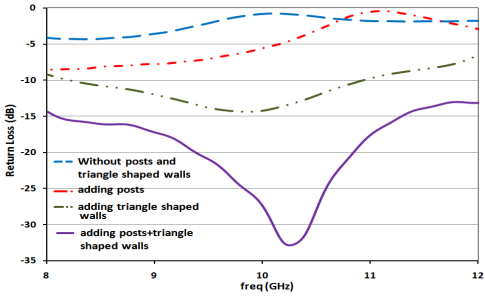

Figure 7. The effects of adding inductive posts and triangle shaped wall to T-junction.

Table 3. The radii and location of the posts in the optimized T-junction.

	R (mm)	Position (x, y)
C1	0.25	11.1, $\pm$5.6
C2	0.6	20.7, 0
C3	0.5	19.1, 0
C4	0.4	17.7, 0
C5	0.25	11.8, $\pm$14.3

Table 4. Design parameters of the Y-junction.

	R (mm)	Position (x, y)
P1	0.25	12.21, $\pm$6.16
L	9	-

3.2. SIW Straight Y-junction

The Y-junction, shown in Figure 8, is used at the output section of the proposed power splitter. The distance L between the output ports' common wall and input port can be optimized in order to achieve a low level of input return loss over a given bandwidth. Meanwhile, to reduce the reflections from the two SIW branches, the posts P1 have been added. By optimizing the positions and diameters of these posts, good performance can be achieved. Design parameters of this junction are shown in Table 4, where R is the radius of P1 posts.

The simulated return loss and insertion loss results of both the T and Y junctions are shown in Figure 9 and the various types of losses are categorized in Table 5.

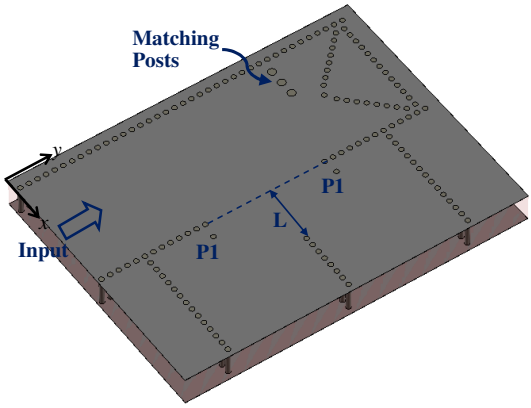

Figure 8. The geometry of the straight Y-junction.

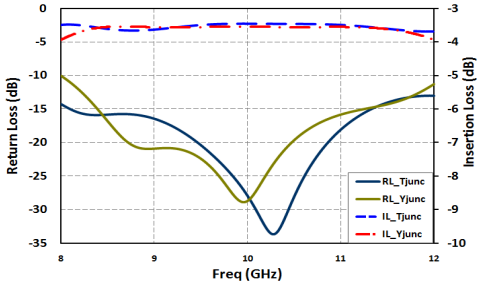

Figure 9. Simulated return loss and insertion loss of T and Y junctions.

Table 5. Summary of the simulated loss results in T and Y-junctions.

Component	T-junc Loss (dB)	Y-junc Loss (dB)
Dielectric loss	0.23	0.23
Copper loss	0.06	0.08
Transition loss	0.2	0.2
Leakage loss	0.08	0.07
Total loss	0.57	0.58

4. EIGHT-WAY X-BAND SIW POWER DIVIDER EXPERIMENTS AND RESULTS

An eight-way X-Band SIW power divider has been designed and fabricated using standard PCB process. The whole structure is

fabricated using a single substrate with $\varepsilon_r = 3.38$, $\tan\delta = 0.0027$ at 10 GHz and thickness of 1.524 mm (RO4003c Rogers) and is shown in Figure 10(a). The divider structure is comprised of 3 optimized T-junctions and 4 Y-junctions. For its insertion loss evaluation we fabricated as well back-to-back structure, as shown in Figure 11(a). The measured insertion loss of the back-to-back structure is less than 2.1 dB, and its input return loss is better than 10 dB over 8 to 12 GHz frequency range. The measured insertion loss of approximately 1.05 dB is better than previously reported results by [1, 4], and [16].

The fabricated divider was measured and the insertion loss results of the divider including the SIW-GCPW transitions and SMA connectors at the input and output ports are shown in Figure 10. It can be seen that the splitter's return loss is better than 10 dB over the 8–12 GHz frequency range, and the measured S_{i1} $(i = 2, 3, \ldots)$ are about -10.4 ± 0.9 dB within the operating frequency range. The measured insertion loss indicates approximately 1.4 ± 0.9 dB loss due to the divider including a 0.2 dB for the output connectors that are not required when the divider is directly connected to the antenna array for

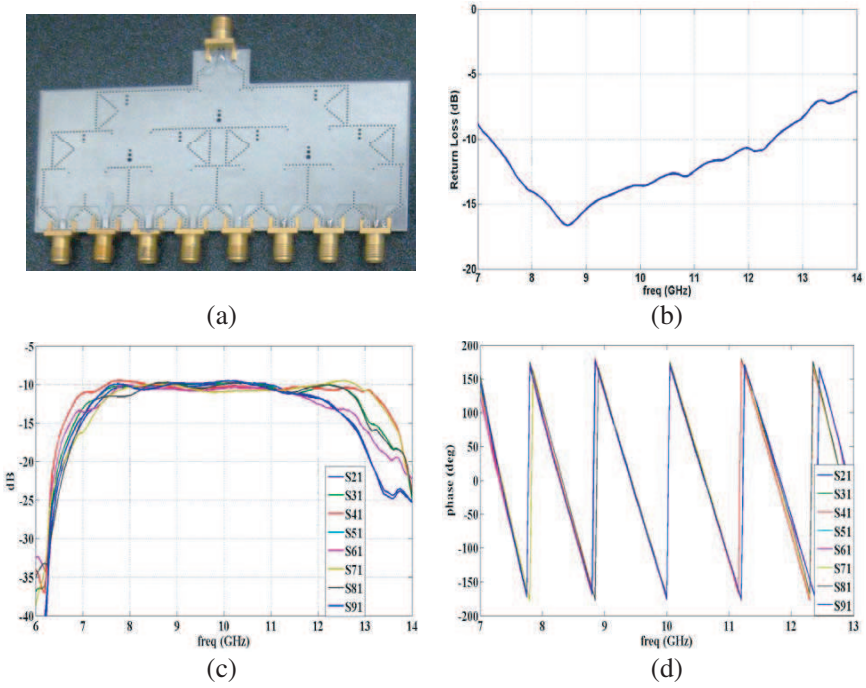

(a) (b) (c) (d)

Figure 10. (a) Manufactured SIW wideband 1×8 power divider. (b) Measured input return loss of SIW power divider. (c) Measured powers at output ports. (d) Output ports' phase.

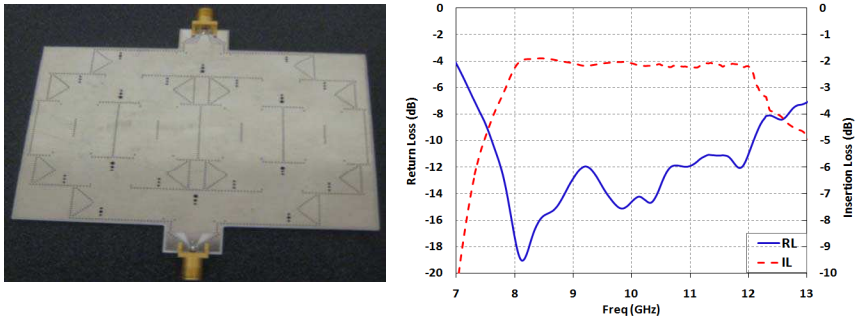

(a) (b)

Figure 11. (a) Back-to-back 1 to 8 feeding network. (b) Measured reflection coefficient and transmission coefficient.

example. The developed SIW power divider provides a balanced power division over a wide bandwidth from 8 to 12 GHz and has successfully demonstrated a maximum of ± 0.9 dB, and $\pm 4^\circ$ amplitude and phase imbalance at the output ports, respectively. The 1 to 8 divider is compact and its whole size is only 10 cm $\times$ 5.5 cm. The measured results are consistent with our simulated results.

5. CONCLUSION

An optimum design of an eight-way X-band planar power divider fed by a GCPW transition has been successfully developed. The compact design has been implemented using SIW technology and is comprised of multitude of optimized T-junctions, Y-junctions, and smooth bends. The input port match has been significantly enhanced by shaping the walls of the T-junctions and inserting multiple posts in strategic locations to smooth out the effects of various discontinuities.

The novel wideband GCPW feed has been developed to improve the performance of the power divider; where a significantly low insertion loss of less than 0.4 dB over a 10 GHz bandwidth has been achieved. The development of a GCPW-SIW transition has helped in obtaining a good input match over an ultra wide frequency range; while preventing higher order mode excitation when using a wide microstrip line feed.

Measurements agreed very well with simulation of the 8-way power divider and demonstrated low return loss over a very wide frequency range using the integrated GCPW transition. The 8-way splitter demonstrated less than ± 0.9 dB, and $\pm 4^\circ$ amplitude and phase imbalance, and insertion loss of approximately 1 dB over 4 GHz

centered at 10 GHz.

The proposed structure has low profile, low insertion loss, wide bandwidth and can be easily integrated into microwave and mm-wave circuits that make it useful for ultra-wide band systems such as diplexers and antenna feeds.

ACKNOWLEDGMENT

The authors gratefully thank Iran Telecommunication Research Center (ITRC) for its helpful support.

REFERENCES

1. Hao, Z., W. Hong, H. Li, H. Zhang, and K. Wu, "Multiway broadband substrate integrated waveguide (SIW) power divider," *IEEE Ant. and Propag. Soc. Int. Symp.*, Vol. 1A, 639–642, 2005.
2. Yang, Y., C. Zhang, S. Lin, and A. Fathy, "Development of an ultra wideband Vivaldi antenna array," *IEEE Ant. and Propag. Soc. Int. Symp.*, Vol. 1A, 606–609, 2005.
3. Germain, S., D. Deslandes, and K. Wu, "Development of substrate integrated waveguide power dividers," *IEEE Canadian Conf. on Elect. and Comp. Eng.*, 1921–1924, 2003.
4. Hao, Z., W. Hong, J. Chen, and K. Wu, "A novel feeding technique for antipodal linearly tapered slot antenna array," *IEEE MTT-S Int. Microw. Symp.*, 1641–1643, 2005.
5. Yang, S., A. Elsherbini, S. Lin, A. Fathy, A. Kamel, and H. Elhennawy, "A highly efficient Vivaldi antenna array design on thick substrate and fed by SIW structure with integrated GCPW feed," *IEEE Ant. and Propag. Int. Symp.*, 1985–1988, 2007.
6. Wu, K., D. Deslandes, and Y. Cassivi, "The substrate integrated circuits — A new concept for high-frequency electronics and optoelectronics," *6th Int. Conf. Telecomm. in Modern Satellite, Cable and Broadcasting Service (TELSIKS)*, Vol. 1, III-X, 2003.
7. Yan, L., W. Hong, K. Wu, and T. J. Cui, "Investigations on the propagation characteristics of the substrate integrated waveguide based on the method of lines," *IEE Proc. Microwaves, Antennas and Propag.*, Vol. 152, No. 1, 35–42, 2005.
8. Djerafi, T., N. J. G. Fonseca, and K. Wu, "Design and implementation of a planar 4×4 butler matrix in SIW technology for wide band high power applications," *Progress In Electromagnetics Research B*, Vol. 35, 29–51, 2011.
9. Zheng, B., Z. Zhao, and Y. Lv, "A K-band SIW filter with bypass coupling substrate integrated circular cavity (SICC) to improved

stopband performance for satellite communication," *Progress In Electromagnetics Research C*, Vol. 17, 95–104, 2010.

10. Qiang, L., Y.-J. Zhao, Q. Sun, W. Zhao, and B. Liu, "A compact UWB HMSIW bandpass filter based on complementary split-ring resonators," *Progress In Electromagnetics Research C*, Vol. 11, 237–243, 2009.
11. Han, S., X.-L. Wang, Y. Fan, Z. Yang, and Z. He, "The generalized Chebyshev substrate integrated waveguide diplexer," *Progress In Electromagnetics Research*, Vol. 73, 29–38, 2007.
12. Zhang, X.-C., Z.-Y. Yu, and J. Xu, "Novel band-pass substrate integrated waveguide (SIW) filter based on complementary split ring resonators (CSRRs)," *Progress In Electromagnetics Research*, Vol. 72, 39–46, 2007.
13. Che, W., E. K.-N. Yung, K. Wu, and X. Nie, "Design investigation on millimeter-wave ferrite phase shifter in substrate integrated waveguide," *Progress In Electromagnetics Research*, Vol. 45, 263–275, 2004.
14. Ismail, A., M. S. Razalli, M. A. Mahdi, R. S. A. Raja Abdullah, N. K. Noordin, and M. F. A. Rasid, "X-band trisection substrate-integrated waveguide quasi-elliptic filter," *Progress In Electromagnetics Research*, Vol. 85, 133–145, 2008.
15. Deslandes, D. and K. Wu, "Analysis and design of current probe transition from grounded coplanar to substrate integrated rectangular waveguides," *IEEE Trans. on MTT*, Vol. 53, No. 8, 2487–2499, 2005.
16. Lin, S., S. Yang, A. E. Fathy, and A. Elsherbini, "Development of a novel UWB Vivaldi antenna array using SIW technology," *Progress In Electromagnetics Research*, Vol. 90, 369–384, 2009.
17. Yang, S., S. H. Suleiman, and A. Fathy, "Low profile multi-layer slotted substrate integrated waveguide (SIW) array antenna with folded feed network for mobile DBS applications," *IEEE Ant. and Propag. Soc. Int. Symp.*, 473–476, 2007.
18. Yang, S. and A. Fathy, "Synthesis of a compound T-junction for a two-way splitter with arbitrary power ratio," *IEEE MTT-S Int. Microw. Symp.*, 985–988, 2005.
19. Yang, S. and A. Fathy, "Design equations of arbitrary power split ratio waveguide T-junctions using a curve fitting approach," *Int. J. of RF and Microw. Computer-Aided Eng.*, Vol. 19, No. 1, 91–98, 2009.
20. Xu, F. and K. Wu, "Guided-wave and leakage characteristics of substrate integrated waveguides," *IEEE Trans. on Microw. Theory and Techniques*, Vol. 53, No. 1, 66–73, 2005.